The Cryosphere Discuss., 5, 1383–1418, 2011
www.the-cryosphere-discuss.net/5/1383/2011/
doi:10.5194/tcd-5-1383-2011

The Cryosphere Discussions

Spatio-temporal measurements and analysis of snow depth in a rock face

V. Wirz[1,2], M. Schirmer[1], S. Gruber[2], and M. Lehning[1]

[1]WSL Institute for Snow and Avalanche Research SLF, Davos, Switzerland
[2]Department of Geography, University of Zurich, Switzerland

Received: 13 April 2011 – Accepted: 21 April 2011 – Published: 6 May 2011

Correspondence to: V. Wirz (vanessa.wirz@geo.uzh.ch)

Published by Copernicus Publications on behalf of the European Geosciences Union.

Abstract

Snow in rock faces plays a key role in the alpine environment for permafrost distribution, snow water storage or run off in spring. However, a detailed assessment of snow depths in steep rock walls has never been attempted. To understand snow distribution in rock walls a high-resolution terrestrial laser scanner (TLS), including a digital camera, was used to obtain snow depth (HS) data with a resolution of one metre. The mean HS, the snow covered area and their evolution in the rock face were compared to a neighbouring smoother catchment and a flat field station at similar elevation. Further we analyzed the patterns of HS distribution in the rock face after different periods and investigated the main factors contributing to them.

In a first step we could show that with TLS reliable information on surface data of a steep rocky surface can be obtained. In comparison to the flatter sites in the vicinity, mean HS in the rock face was lower during the entire winter, but trends of snow depth changes were similar. We observed repeating accumulation and ablation patterns in the rock face, while maximum snow depth loss always occurred at those places with maximum snow depth gain. Further analysis of the main factors contributing to the snow depth distribution in the rock face revealed terrain-wind-interaction processes to be dominant. Processes related to slope angle seem to play a role, but no linear function of slope angle and snow depth was found.

Further analyses should involve measurements in rock faces with other characteristics and higher temporal resolutions to be able to distinguish individual processes better. Additionally the relation of spatial and temporal distribution of snow depth to terrain-wind interactions should be tested.

1 Introduction

Knowledge on spatial and temporal variability of snow depths in alpine terrain is of high importance because snow plays an important role in many alpine environmental aspects, e.g. water management, snow avalanches or permafrost occurrence. The snow distribution in rock faces influences the existence of permafrost (Haeberli, 1996; Keller and Gubler, 1993; Lütschg et al., 2008; Hasler et al., 2011) and contributes to the run off in spring. As rock faces are widespread in alpine environments (e.g., Gruber and Haeberli, 2007), knowledge about the distribution of snow depth in them is important. However, such studies are rare due to the limitations of traditional measurement methods in combination with the inaccessibility and the existence of alpine hazards. By contrast, snow depth distribution in less steep alpine terrain has been studied for many years (e.g., Föhn and Meister, 1983; Cline et al., 1998; Liston and Sturm, 1998; Gauer, 2001; Deems et al., 2006; Doorschot et al., 2001; Mott et al., 2010; Mott and Lehning, 2010) and recent ground temperature trend analyses underline the importance of spatial and temporal snow depth distribution (Zenklusen et al., 2010).

The distribution of snow depth in mountain regions is mainly influenced by the amount of precipitation, solar radiation, air temperature, wind conditions, topography and other processes related to their interactions. On a smaller scale, for example within alpine watersheds, the spatial variability of snow depth is mainly determined by terrain-wind interactions (e.g. Föhn and Meister, 1983, Elder et al., 1991; Luce et al., 1998; Gauer, 2001, Winstral et al., 2002; Raderschall et al., 2008; Lehning et al., 2008) and therefore a lot of effort has been carried out to link snow depths to meteorological (especially wind) and topographic factors (e.g., Blöschl and Kirnbauer, 1992; Anderton et al., 2002; Winstral et al., 2002; Trujillo et al., 2007; Grünewald et al., 2010; Mott et al., 2010).

In steep terrain, such as rock walls, it is to be expected that the spatio-temporal variability of snow depth is not only caused by wind transport but also influenced by processes related to slope angle such as solar radiation and avalanching (including avalanches, sloughs and spindrifts). As knowledge about the snow depth distribution in rock faces is scarce, many hypotheses have been formulated but could so far not been verified properly. Due to the high influence of gravity in steep terrain, different authors assumed that snow cannot accumulate permanently (Winstral et al., 2002; Blöschl and Kirnbauer, 1992; Schmid and Sardemann, 2002). The latter presume that small

TCD
5, 1383–1418, 2011

Spatio-temporal variability of snow depth in a rock face

V. Wirz et al.

sloughs starting from slopes steeper than 55° are frequent while larger avalanches are rare. Another frequent assumption is that with increasing slope angle the snow depth and snow covered area decrease (e.g., Anderton et al., 2002; Machguth, 2006). This assumption has been confirmed by observations in alpine basins at a resolution of 25 m (Blöschl and Kirnbauer, 1992).

Light detection and ranging (LIDAR) altimetry makes it possible to measure area-wide the snow depths with high accuracy, even in inaccessible areas. Airborne laser scanning (ALS) was successfully used in previous studies to determine snow depth distribution in alpine terrain (e.g., Deems et al., 2006; Hopkinson et al., 2001). In the last few years the technique of terrestrial laser scanning (TLS) increased the possibilities to measure snow surfaces with higher spatial and temporal resolution (Bauer and Paar, 2004; Jörg et al., 2006; Prokop, 2008; Schaffhauser et al., 2008; Grünewald et al., 2010). TLS measurements have already been used to obtain precise digital elevation models of rock faces (Bauer et al., 2005; Alba et al., 2005). Until present, TLS has never been applied to investigate the variability of snow depths on rock faces.

In this study we examine TLS measurements to receive snow depth data with a resolution of one metre in a rock face in the eastern Swiss Alps. The aim is to obtain information on (a) the amount of snow depth in the rock face and its temporal evolution compared to flatter sites at similar elevation and in the vicinity, (b) the spatial-temporal variability of snow depths and (c) possible inferences for processes causing this distribution. A strong focus will be on studying probable key factors influencing the snow depth distribution and to investigate how far snow depth distribution is linked to frequently used terrain parameters such as slope, curvature and roughness. Regarding the terrain parameters we assume that in a rock face more snow can probably accumulate in the steep, rough areas than in the steep, smooth ones and that curvature influences both avalanching and wind drift. Finally frequently made hypotheses such as the one that with increasing steepness snow depth decreases and that on slopes steeper than a specific threshold snow cannot accumulate were tested for the rock face on a small scale.

2 Data and methods

2.1 Study site

The main study site Chüpfenflue is a southwest oriented slope in the region of Davos, Eastern Swiss Alps (Fig. 1). The rock face elevation ranges from 2200 to 2658 m a.s.l. The mean slope angle is 42° varying from horizontal to nearly vertical (max. 86°, calculated on a grid of 1 m resolution). The base area (horizontal projected area) of the rock face is about 0.16 km^2, of which approximately 60 % were covered by the TLS measurements. Surrounding the Chüpfenflue, seven automatic weather stations measure wind direction and velocity, air temperature, relative humidity and solar radiation, and several fixed reference points with reflectors are available for referencing the TLS measurements (Fig. 1).

Two sites at similar elevations were used to compare the snow depth in the rock face to more gentle terrain: the nearby Albertibach catchment and the Versuchsfeld Weissfluhjoch. The neighbouring Albertibach is generally smoother, less steep (mean slope of 30°) and includes diverse expositions (data published in Grünewald et al., 2010 and Schirmer et al., 2011). It has a horizontal area of 1.3 km^2 of which 46 % were covered by TLS. The flat field Versuchsfeld Weissfluhjoch (WFJ, 2540 m a.s.l) has one of the longest records of observations worldwide and has been subject to numerous investigations (e.g., Stoessel et al., 2010). For our purpose, snow depth was measured daily at one point (SLF, 2009).

2.2 Weather conditions

The seasonal development of snow depth measured at WFJ during winter 2008/09 was similar to the long-term mean (1934 to 2008) although snow depth was generally higher than average (SLF, 2009). Throughout the accumulation season, snowfalls were predominantly observed in combination with strong northwest winds in the Albertibach catchment and at WFJ. At the end of January, the stations measured snowfall in

TCD
5, 1383–1418, 2011

combination with weak winds, after the collapse of a Föhn event (strong, dry southerly winds). Another Föhn event was responsible for the reduction of snow depth in the region of Davos in the beginning of February. The accumulation season ended at the end of March and was followed by a period of strong ablation. Towards the end of April, the ablation process was interrupted by a period with little snowfall and colder temperatures. In May, ablation was high due to warm temperatures. On 25 May (last measurement), the rock face was nearly snow free, while the Albertibach catchment still had over 30 % snow cover. The Albertibach catchment became snow free at the end of June (Grünewald et al., 2010).

2.3 Measurement methods

The TLS used in this context (Riegl, LPM-321, Table 1) measures distances with a near-infrared signal with a wavelength of 905 nm, ensuring favourable reflectance of the snow (Painter and Dozier, 2003) and little penetration of the laser signal (Prokop, 2008). The density of the resulting point cloud depends on the distance to the object, the inclination angle and the resolution used. The distance, inclination angle and point divergence determine the size of each laser footprint. With distances to the surface ranging from 350 to 700 m and a resolution of 0.36°, the average point density was 6.12 points per square meter. Circular footprints had diameters of 0.14–0.28 m, but were usually enlarged to ellipses where incidence angles were small.

The TLS was positioned next to the weather station WAN2 (Fig. 1), installed on a stable tripod that did not move during one scan and the duration of one single scan was restricted to one hour. Especially at the foot of the face and behind large ridges, gaps in the measured surface resulted from measuring shadows (blind areas, Fig. 1). Additionally, a digital camera (Canon EOS 350D) installed on the TLS, was used to take high-resolution photos during measurements that were ortho-rectified during processing.

The dataset for the main site consists of 14 TLS measurements with snow during the winter 2008/2009 (January–May 2009), one measurement after the first snowfall of

TCD
5, 1383–1418, 2011

the winter 2009/2010 (21 October) and one scan without snow, serving as the digital elevation model (DEM, Table 3). Additionally, two helicopter-based ALS (Vallet et al., 2005; Skaloud et al., 2006) data sets covering the entire area in 2009 were used: one from 9 April and one from 19 September in snow free conditions. The time lag between the TLS measurements of Chüpfenflue and Albertibach was less than two days. In April, no measurements were made in the Albertibach catchment. An overview of the periods used for comparing Chüpfenflue, Albertibach and WFJ is given in Table 2.

2.4 Processing

TLS data were processed with the software RiProfile (Riegl, version, 1.4.3). Measurements were corrected for atmospheric and geometric influences and filtered to achieve a more balanced point density (octree-filter; Riegl, 2005). The measured point cloud was transformed into the Swiss coordinate system CH1903 using seven permanently installed reflectors with known coordinates. To obtain a DEM, point clouds were triangulated using Delauny triangulation within ArcGIS. The maximal edge length of the triangles was limited to 5 m to prevent interpolation in obvious measuring shadows but to ensure that areas of low point density are still triangulated. The resulting triangulated irregular networks (TINs) were converted by a linear interpolation into digital surface models (DSMs) with a grid resolution of one meter. This resolution offered a good compromise between resolution, data storage and the retention of original data points. Snow depth or its changes over time are calculated by subtracting DSM values from differing measurement dates. In this study we use snow depth (HS) referring to the vertical height as it is used to estimate the snow water equivalent (Fierz et al., 2009).

Snow covered area (SCA) is important to understand the distribution of HS, however, using TLS only, it cannot be examined precisely as the snow cover in the rock face is often thin and lies within the uncertainty of the HS data generated by subtraction (see next section). To overcome this, a binary raster mask of SCA for each measurement day was generated manually using a threshold for one of the colour orthophoto RGB channels.

TCD
5, 1383–1418, 2011

To estimate the HS changes only those cells were included which were snow covered at the beginning and at the end of the period analyzed. This restriction facilitates the determination of reliable ablation rates. The pathologic case is excluded in which many pixels may show a small ablation rate for a given time period between TLS measurements, caused by the fact that the pixel was already close to complete ablation at the start of the period. Mean HS is therefore also given with respect to the snow-covered base area. The only exception to this is the comparison with Albertibach and WFJ where mean HS is calculated for the entire base area (HS_{tot}) since the data for SCA was not available in Albertibach.

Based on the summer DEM, slope angle, curvature and surface roughness (VRM; Sappington et al., 2007) were calculated within ArcGIS. As this strongly depends on cell size, we derived terrain parameters at diverse resolutions (1 m, 5 m, 10 m and 25 m) in order to analyze the effects of small vs. bigger terrain features.

2.5 Data quality analysis

Prokop et al. (2008) and Grünewald et al. (2010) quantified the error of snow depth measurements achieved with a similar and an identical terrestrial laser scanning system in alpine terrain and compared it to other established methods such as tachymeter or manual snow probing. Prokop et al. (2008) showed that at distances up to 300 m the mean difference (μ) between the methods was 4.5 cm with a standard deviation (σ) of approximately 2 cm. The measurements carried out by Grünewald et al. (2010) and by Kenner et al. (2011), using the same TLS as in this study yielded similar results (up to 250 m: μ =4 cm and σ =5 cm). These results cannot be transferred directly to the rough and steep surface examined here and tachymeter-based reference measurements without a reflector were impossible due to the large distance between TLS and rock face. We tested our measurements for repeatability (same disposition, unchanged object) on four days and for reproducibility (changed disposition, unchanged object) once for the snow-covered surface and on four days for the snow-free surface.

Additionally, TLS and ALS measurements of the snow free rock face were compared to analyze errors in blind areas of the TLS and to compare both methods.

All repeatability tests showed similar results and we present the results of 17 March only. A mean error of 8.7 cm (mean of the absolute differences, μ_{AE}) together with a standard deviation of 20.3 cm was observed. The offset (μ) was negligible ($\mu = -2.9$ cm). The results of the reproducibility were similar but with slightly larger deviations ($\mu_{AE} = 13$ cm, $\mu = -18.5$ cm and $\sigma = 38$ cm). In most cases, the main differences occurred in the steep, rough parts of the rock face. In those areas, the main deviations between DEMs derived from TLS- and ALS- occurred. The comparison with ALS data confirmed that within blind areas of the TLS it was not possible to interpolate appropriately. The absolute differences between the two DEMs excluding blind areas were on average $\mu_{AE} = 48.2$ cm, $\mu = 38.5$ cm and $\sigma = 81$ cm with elevations based on TLS generally being higher. The offset between both data sets probably resulted from wrong calibration of the reference points. We therefore did not calculate snow depths derived from different LIDAR-methods.

2.6 Explorative data analysis

In an attempt to describe the amount of snow and its temporal evolution in the rock face comparatively, we compare the mean HS_{tot}, the mean HS changes as well as SCA between the rock face and more gentle terrain. The dataset was analyzed visually and with descriptive statistics (histogram, mean μ and standard deviation σ). To describe the variability of HS the coefficient of variation ($CV = \sigma/\mu$) was used. The simple linear regression coefficient of Pearson for two univariate variables was applied to quantify the similarity between different spatial distributions of HS. The Kruskal-Wallis-Test is used to study which factors are relevant for HS patterns. We tested if variability of HS can be explained by a simple terrain parameter using Pearson's coefficient of determination (R) for two univariate variables. We further analyzed if a linear relation exists between slope, curvature and roughness to HS patterns of different periods. As only small ranges of exposition (SSE to W) and elevation (2100 to 2700 m a.s.l.) were measured in the rock face, it was not possible to study the influence of the frequently used parameters exposition and elevation on the snow distribution in the rock face.

3 Results

3.1 Comparison with more gentle terrain

The evolution of mean HS_{tot} at Chüpfenflue, Albertibach and Versuchsfeld Weissfluhjoch (WFJ) were similar (Fig. 2): at all three sites the peak of winter accumulation was reached at the end of March and from January to the end of the accumulation season, the mean HS_{tot} increased by about 50 %. Furthermore, at all three locations a reduction of HS_{tot} occurred at the beginning of February due to a Föhn event. A period with strong ablation at the beginning of April followed the peak of winter accumulation. From the end of March to the end of May the HS_{tot} decreased. In May, when air temperatures measured in the study area stayed above zero degrees nearly daily, the reduction was particularly strong.

Mean HS_{tot} at Chüpfenflue was constantly smaller, with a maximum difference of 1.5 m to WFJ on 1 May and 1.1 m to the Albertibach catchment on 27 March (Fig. 2). At the end of the accumulation season, HS_{tot} at Chüpfenflue was 1.1 m, 2.2 m at Albertibach and 2.4 m at the Versuchsfeld WFJ. Note again that WFJ is a point measurement and the other two are averages over areas. The difference in mean HS_{tot} between the rock face and the other two sites increased with higher HS_{tot} during the accumulation period. During the ablation period, no clear trend was found: the difference to Albertibach decreased, while the difference to the WFJ first increased until the end of April, but finally also decreased towards the end of May.

Regarding changes of HS_{tot} during periods with snowfall, more snow accumulated in the more gently sloping sites than in the rock face, except during the first observation period when snowfall was accompanied by weak wind (Table 2). The highest difference occurred in the last period of the accumulation season: while at Albertibach an

TCD
5, 1383–1418, 2011
Spatio-temporal variability of snow depth in a rock face
V. Wirz et al.

increase in HS_{tot} of 41 cm and at WFJ of 31 cm was measured, HS_{tot} at Chüpfenflue increased only by 13 cm. During the Föhn period in February, the reduction of HS_{tot} in the rock face was comparably higher. During the ablation season at the beginning the reduction of HS_{tot} was mostly higher at the more flat sites, but towards the end of the accumulation season the reduction was greater in the rock face.

Throughout the observation period, SCA in the rock face was at least 10 % lower than at Albertibach (Fig. 3). During the accumulation period in the rock face, at least 20 % of the area remained snow free, at Albertibach maximal 3 %. The highest relative difference in SCA (33 %) between the two sites occurred in the middle of May, when already most of the area in the rock face was snow free (SCA = 11 %).

The spatial variability of HS_{tot} at Chüpfenflue ($1.98 < CV < 4.5$) was at least 30 % higher than at Albertibach ($0.53 < CV < 2.5$) throughout the entire observation period. During the accumulation season the difference was smaller ($maxCV_{diff}$=0.5) than during the ablation period ($maxCV_{diff}$=2.9). In addition, the changes in HS_{tot} were more variable in the rock face than in the Albertibach catchment, except during the first two periods with snowfall in combination with practically no wind, or with a Föhn event (Table 2).

3.2 Snow depth distribution in the rock face

The spatial patterns of HS in the rock face remained similar during the entire winter (Fig. 4). The main snow accumulations occurred in the lee of ridges orientated normal to the prevailing wind direction (northwest), in small gullies, or at the foot of steep rocks. Cells with only a thin snow cover mostly occurred on ridges or around the peak. Those repeating patterns were also expressed in high correlations between the HS distributions of different measurement dates (Table 4) and especially with the patterns of HS_{max}, the HS at the end of the accumulation season ($R > 0.79$) between the two winters studied. The correlations between HS after the first snowfall in winter 2009/10 to HS_{max} of the winter 2008/09 were weaker ($0.37 < R < 0.47$).

Even if the spatial patterns of HS were similar during the entire observation period, the distribution of HS changes during one single observation period varied, depending on weather conditions (e.g. snow fall in combination with strong north westerly wind vs. snow fall with weak wind). During the accumulation season, periods with snowfall accompanied by strong wind were most frequent (Table 3). The patterns of HS changes during those periods were similar (Fig. 5 and Table 5) and correlated well with the spatial distribution of HS_{max} (Table 5). During a period with snowfall and weak winds (16 to 28 January) the distribution of HS changes showed a more homogeneous pattern and lower variability (CV=0.62, Table 3). In comparison with periods with strong winds ($CV_{min} = 1.22$), snow accumulated more regularly, no particular accumulation zones were established and areas, which normally stayed snow free during snowfalls, became snow covered (highest SCA on 28 January, Fig. 3). The distribution of HS after the snowfall event with no wind did not correlate well with HS_{max} ($R = 0.18$) or HS change ($|R|_{max} = -0.17$); but it correlated negatively to the negative HS changes in February due to a Föhn event ($R = -0.55$).

During the ablation season the patterns of changes in HS were mainly influenced by the distribution of the persisting snow depth. Where HS_{max} was high, its reduction was stronger (Fig. 5). These observations were confirmed by strong negative correlations of HS changes with HS_{max} ($-0.55 < R < -0.31$, Table 5) as well as by a Kruskal-Wallis-test (Fig. 8).

3.3 Interrelation with terrain features

The correlation analysis between snow distributions and terrain parameters showed similar results for all cell sizes (Table 6). Only weak correlations between changes in HS or absolute HS and slope angle ($|R|_{max} = 0.13$), curvature ($|R|_{max} = 0.21$) and surface roughness ($|R|_{max} = 0.21$) were found. Correlations were particularly small ($|R|_{max} = 0.09$) during the ablation season. The results of a Kruskall-Wallis-Test support that slope has nearly no influence on the amount of negative HS changes (Fig. 8).

Even though correlations between terrain parameters and HS were weak, snow-covered cells at the end of the accumulation period differed significantly from the snow-free cells with regard to slope angle and surface roughness (Fig. 8). The snow-covered cells at the end of the accumulation season were significantly less steep and rough. Note that steepness and roughness have been determined from the summer DTM as described above. On the other hand, at the end of the accumulation period nearly 40 % of the snow covered cells had slope angles between 35° and 40°, but less than 5 % of the snow covered cells had slope angles lower than 30° (Fig. 6). The highest HS_{max} in the rock face occurred in areas around 40° and not in flat parts of the rock face as may have been expected. Cells with slope angles between 35° and 40° had an average HS_{max} of 1.5 m. The mean HS_{max} of cells with a slope angle lower than 30° was only around 1 m, similar to the mean HS_{max} of cells with a steepness between 60° and 70°. The distribution of slope angles in the rock face is not uniform and only few cells have slope angles below 30° or higher than 70° (Fig. 7, right axis).

The influence of slope angles on SCA was examined independently of their distribution (Fig. 7). The highest SCA occurred around 40°, where HS was largest (Fig. 6). Nevertheless, 70 % of the cells with slope angles between 50° and 55° and 50 % of those with slope angles between 60° and 65° were snow covered. However, in classes with slope angles lower than 30° up to 50 % of the cells remain snow free. Most of the near-horizontal areas in the rock face occur on wind-exposed ridges or close to the summit, where airflow often accelerates. This may explain the high proportion of gently-sloping snow free cells.

To confirm the hypothesis that snowfall events with weak wind lead to higher SCA than those with a strong northwest-wind, snowfalls with differing wind conditions were investigated. SCA was higher after snowfalls in calm conditions than after those with strong wind, at least in areas with slope angles between 20° and 80° (Fig. 7). The two curves differ mostly between 45° and 70° and show that snowfalls in calm conditions resulted in accumulation in steeper and rougher areas.

4 Discussion

4.1 Factors influencing the distribution of HS

During the entire observation season, the spatial patterns of HS remained similar although HS changes between periods differed depending on weather conditions. Strong wind dominated snowfall events and led to accumulation patterns in those periods, which correlated strongly with HS distribution at the end of the accumulation season. The distribution of HS is therefore strongly controlled by snowfall in combination with strong winds. Schirmer et al. (2011) made similar observations during the accumulation period in winter 2008/09 in the Albertibach catchment. The timing of melt out was mostly dominated by the characteristics of those accumulations (cf. Grünewald et al., 2010; Anderton et al., 2002; Luce et al., 1998). Correlations between HS and its changes with terrain parameters were generally weak and the correlation coefficients between HS at the end of the accumulation season and terrain parameters were similar to those of previous studies in smoother terrain (e.g., Anderton et al., 2002; Winstral et al., 2002). Correlations were weaker during ablation than during accumulation (cf. Blöschel and Kirnbauer, 1992). The hypothesis that rough terrain tends to accumulate more snow is not supported (Fig. 8). Similarly, the hypotheses that snow cannot permanently accumulate at slope angles greater than a threshold (e.g., $>60^{\circ}$) due to avalanching is not supported (Fig. 7). We indeed found half of the cells were snow-covered in steep parts ($>60^{\circ}$) of the rock face and during the entire measurement period no avalanches or small sloughs were observed. This may be a result of the particular surface geometry of this rock face. A general decrease of HS with increasing slope angle is not confirmed by our data, either (Fig. 7). However, SCA at the end of the accumulation season was markedly less steep (median $= 39^{\circ}$) than the snow free area (median $= 44^{\circ}$). The comparison with previous studies that found a decrease in SCA with increasing slope (e.g., Blöschl and Kirnbauer, 1992) is difficult because they used coarser DEMs in terrain that was generally smoother than that in this study.

TCD
5, 1383–1418, 2011

Spatio-temporal variability of snow depth in a rock face

V. Wirz et al.

It appears that terrain-wind interactions played a major role in the rock face because the main accumulation zones were in the lee behind ridges (Fig. 4), highest HS occurred in areas with a steepness between 30° and 55°, comparably little snow was accumulated during periods with strong winds and flat areas were mostly snow free due to wind-drift.

4.2 Reasons for reduced HS in the rock face

Compared to the more gently sloping sites, the rock face is characterized by smaller mean HS_{tot} and SCA as well as a higher variability of HS_{tot} (Fig. 2, Table 2 and Fig. 3). A possible reason for smaller HS_{tot} is higher snow density. The transport of snow by avalanching (which was not observed) or wind usually increases its density. Other possible reasons for the reduced HS_{tot} could include higher solar radiation input due to the topography or lower albedo (snow free areas) or evacuation of mass by avalanching and wind drift, and are discussed below.

As in previous studies (e.g., Lapen and Martz, 1996; Esseroy and Pomeroy, 2004; Grünewald et al., 2010) we observed that borders of snow patches became snow free earlier than their centre parts and that areas with patchy snow cover became snow-free earlier than those with continuous snow cover. The faster meltout could be caused by the thinner snow cover at the borders or by the smaller albedo of the snow free areas with an associated transport of sensible heat to the borders of the snow patches. The southwest exposure of the measured rock face may additionally promote these effects. The quantification of the effective difference in the reduction of HS at the borders compared to the central parts of the patches was not possible due to the limitations of the temporal resolution of our measurements. If HS_{tot} mean in the rock face was compared to an area inside the Albertibach catchment with similar exposition and slope angles, but generally much gentler and smoother terrain, the mean HS_{tot} and SCA in the rock face were still smaller; and the difference was similar to that in the entire Albertibach catchment. In addition we observed that within the rock face cells with comparably higher decrease in HS did only slightly differ from those with low changes regarding slope angle (Fig. 8). The influence of varying topography and lower albedo on smaller HS_{tot} could therefore not be shown in our analysis. For an improved understanding of processes related to solar radiation additional measurements with higher temporal resolution in rock faces with a larger range of expositions would be necessary.

Mean HS_{tot} in the rock face including the foot of slope where avalanches deposits would accumulate, was compared to the mean HS_{tot} in the Albertibach catchment. HS_{tot} were calculated based on the ALS measurements of 9 April. Excluding the slope foot the mean HS_{tot} in the rock face was 0.6 m ($\sigma = 1.48$ m). Including the slope foot the mean snow depth was 0.8 m ($\sigma = 1.38$ m). In comparison to the HS_{tot} in the Albertibach catchment ($\mu = 138$ cm, $\sigma = 108$ cm) this was still almost 50 % less. But a higher density of the deposited snow due to avalanching (e.g., Elder et al., 1998) could not have been considered because of the inaccessibility. It seems that avalanching contributed to causing a smaller HS_{tot} in the rock face but was not the main reason; this was confirmed by the fact that no avalanching was observed during the entire observation period. Due to the fact that during periods with strong winds, e.g. from 18 to 27 March, comparably less snow was accumulated in the rock face than in the other two sites (70 % less), while during a period with nearly no wind more snow accumulated in the rock face (+10 %), period from 16 to 28 January, we assume that wind transport may play a significant role. The observations suggest that total precipitation of snow per square meter horizontal surface is significantly reduced in the rock face compared to the neighbouring Albertibach. This supports the hypothesis that larger scale transport, which has been defined and described as preferential deposition by Lehning et al., 2008, accounted to a major part for the smaller HS_{tot} inside the rock face observed.

5 Conclusions

It was found that TLS is a suitable method for measuring snow-covered surfaces in steep and rough terrain with high temporal and spatial resolution.

TCD
5, 1383–1418, 2011

Mean HS_{tot} and SCA in the rock face were lower during the entire winter compared to point measurements in a flat area and to TLS measurements in a smoother neighbouring catchment. The temporal evolution of mean HS_{tot} was similar at all three sites. Decreases in HS, especially during ablation periods, were generally stronger; increases generally smaller.

The distribution of HS in the rock face showed similar patterns during the entire observation period. Minima and maxima of HS always occurred in the same spots, even if distributions of HS change differed, depending on weather conditions. The main accumulation zones were in the lee behind ridges, orientated normal to the main wind direction. The distribution of HS_{max} was mainly determined by snowfall in combination with strong northwest winds. Decreases of HS were stronger at places where HS was higher, yet these zones remained snow-covered the longest in spring.

Linear correlations between HS distributions and simple terrain parameters of the underlying topography were weak. Snow covered cells were generally smoother and less steep, but highest SCA and HS occurred at slopes with angles of approximately 40° and not in the flattest parts of the rock face. On this small-scale we could not observe a decrease of HS or SCA with increasing slope angle and snow accumulated permanently even in very steep ($>50°$) terrain. More than 25 % of the area, which was snow covered during the observed period in the accumulation season, was steeper than 50°. Terrain-wind interactions were likely the main factors influencing the variability of HS inside the rock face observed. In particular the total mass balance of the entire face compared to the Albertibach area suggests larger scale transport compatible with the idea of preferential deposition (Mott et al., 2010). Avalanching and slope-angle-dependent solar radiation played a minor role.

This study gives a first overview of HS in a rock face but it is a small rock face with a narrow range of expositions and altitude and only the HS development of one season was measured. We therefore expect that results may differ for other rock faces with different characteristics. To increase knowledge on processes contributing to the HS distribution in a rock face further measurements in rock faces with other characteristics

TCD
5, 1383–1418, 2011

as well as higher temporal resolution would help, as well as information about snow density. To describe the spatial HS distribution in a rock face the influence of wind-terrain-interactions should be investigated. Possibilities would be physically-based energy-wind-models (e.g., Mott et al., 2009) or parameterizations of wind-exposure such as the one formulated by Winstral et al. (2002).

Acknowledgement. This work was funded by the Swiss National Science Foundation and the Swiss Federal Office of the Environment. This study would not have been possible to carry out without the help in the field provided by Luca Egli, Yvonne Schaub, Thomas Grünewald, Rebecca Mott and other colleagues at SLF. Special thanks are dedicated to Thomas Grünewald, Lorenz Böckli and Andreas Hasler for fruitful discussions and valuable comments. In addition, we would like to thank Marcia Phillips, who polished the English.

References

Alba, M., Longoni, L., Papini, M., Roncoroni, F., and Scaioni, M.: Feasibility and problems of TLS in modeling rock faces for hazard mapping, International Society for Photogrammetry and Remote Sensing, WG III/3 Workshop "Laser scanning 2005", Enschede, the Netherlands, September 12–14, 2005.

Anderton, S., Withe, S., and Alvera, B.: Micros-scale spatial variability and the timing of snow melt runoff in a high mountain catchment, J. Hydrol., 268, 158–176, doi:10.1016/S0022-1694(02)00179-8, 2002.

Bauer, A., Paar, G., and Kaltenboeck, A.: Mass movement monitoring using terrestrial laser scanner for rock fall management, in: Geo-information for Disaster Management, edited by: van Oosterom, P., Zlatanova, S., and Fendel, E., Springer, Berlin, 393–406, 2005.

Blöschl, G. and Kirnbauer, R.: An analysis of snow cover patterns in a small alpine catchment, Hydrol. Process., 6, 99–109, 1992.

Cline, D., Bales, R., and Dozier, J.: Estimating the spatial distribution of snow in mountain basins using remote sensing and energy balance modeling, Water Resour. Res., 34(5), 1275–1285, 1998.

Deems, J., Fassnacht, S., and Elder, K.: Fractal distribution of snow depth from LiDAR data, J. Hydrometeorol., 7(2), 285–297, 2006.

DeBeer, C. and Pomeroy, J.: Modelling snow melt and snowcover depletion in a small alpine cirque, Canadian Rocky Mountains, Hydrol. Proc., 23(18), 2584–2599, doi:10.1002/hyp.7346, 2009.
Doorschot, J., Raderschall, N., and Lehning, M.: Measurements and one-dimensional model calculations of snow transport over a mountain ridge, Ann. Glac., 32, 153–158, 2001.
Elder, K., Dozier, J., and Michaelsen, J.: Snow accumulation and distribution in an alpine watershed, Water Resour. Res., 27, 1541–1552, doi:10.1029/91WR00506, 1991.
Elder, K., Rosenthal, W., and Davis, R. E.: Estimating the spatial distribution of snow water equivalence in a montane watershed, Hydrol. Process., 12, 1793–1808, 1998.
Essery, R. and Pomeroy, J.: Implications of spatial distributions of snow mass and melt rate for snow-cover depletion: theoretical considerations, Ann. Glaciol., 38, 261–265, doi:10.3189/172756404781815275, 2004.
Fierz, C., Armstrong, R. L., Durand, Y., Etchevers, P., Greene, E., McClung, D. M., Nishimura, K., Satyawali, P. K., and Sokratov, S. A.: The International Classification for Seasonal Snow on the Ground, IHP-VII Technical Documents in Hydrology N°83, IACS Contribution N°1, UNESCO-IHP, Paris, 2009.
Föhn, P. and Meister, R.: Distribution of snow drifts on ridge slope: measurements and theoretical approximations, Ann. Glac., 4, 52–57, 1983.
Gauer, P.: Numerical modeling of blowing and drifting snow in Alpine terrain, J. Glaciol., 47(156), 97–110, doi:10.3189/172756501781832476, 2001.
Gruber, S. and Haeberli, W.: Permafrost in steep bedrock slopes and its temperature-related destabilization following climate change, J. Geophys. Res., 112, F02S18, doi:10.1029/2006JF000547, 2007.
Grünewald, T., Schirmer, M., Mott, R., and Lehning, M.: Spatial and temporal variability of snow depth and ablation rates in a small mountain catchment, The Cryosphere, 4, 215–225, doi:10.5194/tc-4-215-2010, 2010.
Haeberli, W.: Die Permafrost-Faustregeln der VAW/ETHZ einige grundsätzliche Bemerkungen. Simulation der Permafrostverbreitung in den Alpen mit geographischen Informationssystemen, in: Arbeitsbericht NFP31, vdf-Hochschulverlag, 13–18, 1996.
Hasler, A., Gruber, S., and Haeberli, W.: Temperature variability and thermal offset in steep alpine rock and ice faces, The Cryosphere Discuss., 5, 721–753, doi:10.5194/tcd-5-721-2011, 2011.
Hopkinson, C., Sitar, M., Chamser, L., and Treit, P.: Mapping snowpack depth beneath forest

canopies using airborne lidar, Photogramm. Eng. R. Sens., 70, 323–330, 2004.
Jörg, P., Fromm, R., Sailer, R., and Schaffhauser, A.: Measuring snow depth with a terrestrial laser ranging system, Proceedings for International Snow Science Workshop (ISSW), Telluride, USA, 452–460, 2006.
Keller, F. and Gubler, H.: Interaction between snow cover and high mountain permafrost: Murtèl/Corvatsch, Swiss Alps, in: Proceedings of the Sixth International Conference on Permafrost, 332–337, 1993.
Kenner, R., Phillips, M., Danioth, C., Denier, C., Thee, P., and Zgraggen, A.: Investigation of rock and ice loss in a recently deglaciated mountain rock wall using terrestrial laser scanning: Gemsstock, Swiss Alps, submitted to Cold Reg. Sci. Technol., in press, 2011.
Lapen, D. and Martz, L.: An integrated system of the spatial association between snow depth and topography in a prairie agricultural landscape using digital terrain analysis, J. Hydrol., 184, 277–298, 1996.
Lehning, M., Völksch, I., Gustafsson, D., Nguyen, T., Stähli, M., and Zappa, M.: Alpine3D: A detailed model of mountain surface processes and its application to snow hydrology, Hydrol. Proc., 20, 2111–2128, doi:10.1002/hyp.6204, 2006.
Lehning, M., Löwe, H., Ryser, M., and Raderschall, N.: Inhomogeneous precipitation distribution and snow transport in steep terrain, Water Resour. Res., 44, W07404, doi:10.1029/2007WR006545, 2008.
Liston, G. and Sturm, M.: A snow-transport model for complex terrain, J. Glaciol., 44, 498–516, 1998.
Lütschg, M., Lehning, M., and Haeberli, W.: A sensitivity study of factors influencing warm/thin permafrost in the Swiss Alps, J. Glaciol., 54, 696–704, doi:10.3189/002214308786570881, 2008.
Luce, C., Tarboton, D., and Cooley, K.: The influence of the spatial distribution of snow on basin-averaged snowmelt, Hydrol. Proc., 12, 1671–1683, 1998.
Machguth, H., Paul, F., Hoelzle, M., and Haeberli, W.: Distributed glacier mass-balance modelling as an important component of modern multi-level glacier monitoring, Ann. Glac. 43, 335–343, doi:10.3189/172756406781812285, 2006.
Mott, R. and Lehning, M.: Meteorological modelling of very high resolution wind fields and snow deposition for mountains, J. Hydromet., 11, 934–949, doi:10.1175/2010JHM1216.1, 2010.
Mott, R., Schirmer, M., Bavay, M., Grünewald, T., and Lehning, M.: Understanding snow-transport processes shaping the mountain snow-cover, The Cryosphere, 4, 545–559,

doi:10.5194/tc-4-545-2010, 2010.
Painter, H. and Dozier, J.: The effect of anisotropic reflectance on imaging spectroscopy of snow properties, R. Sens. Environ., 89, 409–422, doi:10.1016/j.rse.2003.09.007, 2004.
Prokop, A.: Assessing the applicability of terrestrial laser scanning for spatial snow depth measurements, Cold Reg. Sci. Technol., 53(3), 155–163, doi:10.1016/j.coldregions.2008.07.002, 2008.
Prokop, A., Schirmer, M., Rub, M., Lehning, M., and Stocker, M.: A comparison of measurement methods: terrestrial laser scanning, tachymetry and snow probing, for the determination of the spatial snow depth distribution on slopes, Ann. Glaciol., 49, 210–216, doi:10.3189/172756408787814726, 2008.
Raderschall, N., Lehning, M., and Schär, C.: Fine scale modelling of the boundary layer wind field over steep topography, Wat. Resour. Res., 44, W09425, doi:10.1029/2007WR006544, 2008.
Riegl: User manual of the Riegl Laser measurement systems and of the software package, 2005.
Sappington, M., Longshore, K., and Thompson, D.: Quantifying landscape ruggedness for animal habitant analysis: a case study using bighorn sheep in the Mojave Desert, J. Wildlife Manage., 71 (5), 1419–1426, doi:10.2193/2005-723, 2007.
Schaffhauser, A., Adams, M., Fromm, R., Jörg, P., Noferini, L., and Sailer, R.: Remote sensing based retrieval of snow cover proprieties, Cold Reg. Sci. Technol., 54 (3), 165–175, 2008.
Schirmer, M., Wirz, V., Clifton, A., and Lehning, M.: Persistence in Intra-annual Snow Depth Distribution. Part I: Measurements and Topographic Control, submitted to Water Resour. Res., 2011.
Schmid, U. and Sardemann, S.: High frequency avalanches: release characteristics and run out distances, Cold Reg. Sci. Technol., 37 (3), ISSW 2002: International Snow Science Workshop, November 2003, 439–451, ISSN 0165-232X, doi:10.1016/S0165-232X(03)00083-1, 2003.
Schmidt, S., Weber, B., and Winiger, M.: Analyses of seasonal snow disappearance in an alpine valley from micro- to meso-scale (Loetschental, Switzerland), Hydrol. Process., 23, 1041–1051, doi:10.1002/hyp.7205, 2009.
Skaloud, J., Vallet, J., Keller, K., Veyssière, G., and Kölbl, O.: An eye for landscapes – rapid aerial mapping with handheld sensors, GPS World, 17, 26–32, 2006.
SLF: Schnee und Lawinen in den Schweizer Alpen Winter 2008/09. Wetter Schnee und La-

winengefahr, Jahresbericht des Winters 2008/09, WSL-Institut für Schnee- und Lawinenforschung, SLF, 2009.
Stoessel, F., Manes, C., Guala, M., Fierz, C., and Lehning, M.: On the micrometeorology of surface hoar on mountain snow covers, Water Resour. Res., doi:10.1029/2009WR008198, 2010.
Trujillo, E., Ramirez, J., and Elder, K.: Topographic, meteorologic and canopy controls on the scaling characteristics of the spatial distribution of snow depth, Water Resour. Res., 43, W07409, doi:10.1029/2006WR005317, 2007.
Vallet, J. and Skaloud, J.: Helimap: Digital imagery/lidar handheld airborne mapping system for natural hazard monitoring, in: 6th Geomatic Week, Barcelona, Spain, 2005.
Winstral, A., Elder, K., and Davis, R.: Spatial snow modelling of wind-redistributed snow using terrain-based parameters, J. Hydrometeorol., 3, 524–538, 2002.
Winstral, A. and Marks, D.: Simulating wind fields and snow redistribution using terrain-based parameters to model snow accumulation and melt over a semi-arid mountain catchment, Hydrol. Proc., 16, 3585–36, 2002.
Zenklusen, E., Blanchet, J., and Phillips, M.: Analysis of ground temperature trends in Alpine permafrost using generalized least squares, J. Geophys. Res. 115, F04009, doi:10.1029/2009JF001648, 2010.

TCD
5, 1383–1418, 2011

Spatio-temporal variability of snow depth in a rock face

V. Wirz et al.

Table 1. Technical features of the used long rang laser measuring systems (LPM-321; Riegl, 2005).

Parameter	Value
Principle	Time-of-flight
Wavelength	905 nm
Pulsrate	20 000 Hz
Beam spread angle	0.8 mrad
Max. range, with reflectance $<80\%$ and 1000 Hz	1500 m
Used resolution for finescans	0.36°
Accuracy	$25\,\mathrm{mm} \pm 20\,\mathrm{ppm}$

TCD
5, 1383–1418, 2011

Table 2. Snow depth change (dHS) at the Versuchsfeld Weissfluhjoch (WFJ), the Chüpfenflue (Chüpfen.) and the Albertibach catchment (Albertib.) and their variability (CV).

	WFJ	Chüpfen.		Albertib.	
Date	dHS	dHS	CV	dHS	CV
16 Jan–28 Jan 2009	0.32	0.28	0.62	0.25	0.78
29 Jan–3 Feb 2009	−0.08	−0.13	−0.93	−0.10	−1.02
4 Feb–4 Mar 2009	0.46	0.32	1.22	0.41	1.32
5 Mar–17 Mar 2009	0.22	0.16	1.45	0.24	1.08
18 Mar–27 Mar 2009	0.31	0.13	1.78	0.41	0.74
28 Mar–31 Mar 2009	−0.13	−0.05	−3.43	−0.10	−1.62
1 Apr–1 May 2009	−0.37	−0.72	−0.75	−0.81	−0.50
2 May–15 May 2009	−0.38	−0.32	−1.44	−0.52	−0.31
16 May–20 May 2009	−0.21	−0.35	−0.61	−0.33	−0.33
21 May–25 May 2009	−0.31	−0.63	−0.30	−0.45	−0.29

TCD
5, 1383–1418, 2011

Table 3. Observation periods in the southwest face of the Chüpfenflue: name of the period, date, mean snow depth change (dHS), snow depth at the end of the period (HS_{end}), coefficient of variation of the snow depth change (CV dHS) and coefficient of variation of HS_{end} (CV HS_{end}) and the main weather situation.

Periods	Date	dHS	HS_{end}	CV dHS	CV HS_{end}	Weather situation
DGM	23 Aug 2008					Snow free
Period 1	16 Feb–28 Feb 2009	0.28	0.80	0.62	0.68	Snowfall with weak wind
Period 2	28 Jan–3 Feb 2009	−0.13	0.67	−0.93	0.79	Föhn event
Period 3	3 Feb–4 Mar 2009	0.32	0.96	1.22	0.81	Snowfall with NW-wind
Period 4	4 Mar–17 Mar 2009	0.16	1.14	1.45	0.80	Snowfall with NW-wind
Period 5	17 Mar–27 Mar 2009	0.13	1.28	1.78	0.84	Snowfall with NW-wind
Period 0	Oct 2009	0.18	1.30	1.77	0.77	Snowfall with NW-wind
Period 6	27 Mar–31 Mar 2009	−0.05	0.94	−3.43	0.90	HS reduction
Period 7	31 Mar–15 Apr 2009	−0.89	0.84	−0.34	1.01	HS reduction
Period 8	15 Apr–24 Apr 2009	−0.19	0.53	−0.81	1.51	HS reduction
Period 9	24 Apr–1 May 2009	0.06	0.80	2.42	1.11	Snowfall & HS reduction
Period 10	1 May–7 May 2009	−0.13	0.59	−1.26	1.36	HS reduction
Period 11	7 May–15 May 2009	−0.56		−0.56		HS reduction
Period 12	15 May–20 May 2009	−0.35	0.77	−0.61	1.08	HS reduction
Period 13	20 May–25 May 2009	−0.63	0.84	−0.3	0.88	HS reduction
Period 0	Oct 2009	0.18	1.30	1.77	0.77	Snowfall with NW-wind

TCD
5, 1383–1418, 2011

Table 4. Pearson's Correlation coefficients between snow depth (HS) distributions in the rock face Chüpfenflue on different days in 2009.

Date	16 Jan	28 Jan	2 Mar	4 Mar	17 Mar	27 Mar	31 Mar	ALS	15 Apr	24 Apr	1 May	7 May	15 May	20 May	25 May	21 Oct
16 Jan	1	0.95	0.94	0.89	0.86	0.83	0.84	0.78	0.78	0.8	0.82	0.8	0.73	0.68	0.54	0.69
28 Jan	0.95	1	0.95	0.9	0.87	0.82	0.83	0.67	0.75	0.76	0.77	0.75	0.68	0.61	0.47	0.58
2 Mar	0.94	0.95	1	0.88	0.84	0.79	0.79	0.59	0.72	0.74	0.75	0.73	0.7	0.62	0.5	0.55
4 Mar	0.89	0.9	0.88	1	0.97	0.95	0.95	0.65	0.9	0.88	0.86	0.88	0.82	0.78	0.77	0.53
17 Mar	0.86	0.87	0.84	0.97	1	0.98	0.98	0.85	0.95	0.95	0.92	0.95	0.89	0.89	0.87	0.55
27 Mar HS_{max}	0.83	0.82	0.79	0.95	0.98	1	0.99	0.72	0.93	0.92	0.89	0.91	0.83	0.81	0.8	0.47
31 Mar	0.84	0.83	0.79	0.95	0.98	0.99	1	0.74	0.95	0.94	0.91	0.93	0.86	0.85	0.83	0.47
ALS 9 Apr	0.78	0.67	0.59	0.65	0.85	0.72	0.74	1	0.81	0.88	0.77	0.81	0.75	0.8	0.91	0.37
15 Apr	0.78	0.75	0.72	0.9	0.95	0.93	0.95	0.81	1	0.98	0.97	0.97	0.9	0.88	0.87	0.52
24 Apr	0.8	0.76	0.74	0.88	0.95	0.92	0.94	0.88	0.98	1	0.98	0.98	0.95	0.94	0.93	0.54
1 May	0.82	0.77	0.75	0.86	0.92	0.89	0.91	0.77	0.97	0.98	1	0.98	0.93	0.9	0.92	0.53
7 May	0.8	0.75	0.73	0.88	0.95	0.91	0.93	0.81	0.97	0.98	0.98	1	0.94	0.92	0.93	0.52
15 May	0.73	0.68	0.7	0.82	0.89	0.83	0.86	0.75	0.9	0.95	0.93	0.94	1	0.97	0.97	0.52
20 May	0.68	0.61	0.62	0.78	0.89	0.81	0.85	0.8	0.88	0.94	0.9	0.92	0.97	1	0.97	0.53
25 May	0.54	0.47	0.5	0.77	0.87	0.8	0.83	0.91	0.87	0.93	0.92	0.93	0.97	0.97	1	0.33
21 Oct	69	0.58	0.55	0.53	0.55	0.47	0.47	0.37	0.52	0.54	0.53	0.52	0.52	0.53	0.33	1

TCD
5, 1383–1418, 2011

Spatio-temporal variability of snow depth in a rock face

V. Wirz et al.

Table 5. Pearson's Correlation coefficients between distributions of snow depth change (dHS) of different observation periods and snow depth at the end of the accumulation season (HS_{max}). Periods are described in Table 3.

Period	1	2	3	4	5	6	7	8	9	10	11	12	13	0	HS_{max}
1	1	−0.55	0.1	0.08	0.01	−0.17	−0.08	−0.13	−0.01	−0.06	−0.2	0.04	0.1	−0.06	0.18
2	−0.55	1	−0.28	−0.2	−0.14	0.03	0.17	0.05	0.05	0.06	0.31	0.09	0.04	−0.03	−0.22
3	0.1	−0.28	1	0.56	0.48	−0.44	−0.51	−0.33	−0.02	−0.06	−0.42	−0.33	−0.25	0.3	0.82
4	0.08	−0.2	0.56	1	0.45	−0.47	−0.48	−0.33	0	0.04	−0.33	−0.31	−0.24	0.28	0.74
5	0.01	−0.14	0.48	0.45	1	−0.62	−0.45	−0.27	−0.01	0.06	−0.34	−0.21	−0.3	0.19	0.63
6	−0.17	0.03	−0.44	−0.47	−0.62	1	0.38	0.33	0.04	0.06	0.4	0.18	0.17	−0.07	−0.43
7	−0.08	0.17	−0.51	−0.48	−0.45	0.38	1	0.26	0.03	0.14	0.51	0.22	0.24	−0.12	−0.55
8	−0.13	0.05	−0.33	−0.33	−0.27	0.33	0.26	1	−0.28	−0.01	0.34	0.12	0.2	−0.01	−0.31
9	−0.01	0.05	−0.02	0	−0.01	0.04	0.03	−0.28	1	−0.31	−0.14	−0.02	0.1	0.04	0.04
10	−0.06	0.06	−0.06	0.04	0.06	0.06	0.14	−0.01	−0.31	1	−0.17	0.09	0.08	0	−0.06
11	−0.2	0.31	−0.42	−0.33	−0.34	0.4	0.51	0.34	−0.14	−0.17	1	0.21	0.07	−0.12	−0.51
12	0.04	0.09	−0.33	−0.31	−0.21	0.18	0.22	0.12	−0.02	0.09	0.21	1	0.17	−0.23	−0.47
13	0.1	0.04	−0.25	−0.24	−0.3	0.17	0.24	0.2	0.1	0.08	0.07	0.17	1	−0.24	−0.45
0	−0.06	−0.03	0.3	0.28	0.19	−0.07	−0.12	−0.01	0.04	0	−0.12	−0.23	−0.24	1	0.47
Hs_{max}	0.18	−0.22	0.82	0.74	0.63	−0.43	−0.55	−0.31	0.04	−0.06	−0.51	−0.47	−0.45	0.47	1

TCD
5, 1383–1418, 2011

Spatio-temporal variability of snow depth in a rock face

V. Wirz et al.

Table 6. Pearson's Correlation coefficients between snow depth (HS) on different days in 2009 or HS change distributions of different periods (see Table 3) with terrain parameters, calculated from DHMs with different cellsizes.

Slope	DHM 1 m	DHM 2 m	DHM 5 m	DHM 10 m	DHM 25 m
Period 5	−0.06	−0.04	−0.03	−0.08	−0.01
Period 1	0.08	0.04	0.07	0.13	0.06
Period 2	−0.08	−0.03	−0.07	−0.1	−0.03
Period 11	0	0.06	0	0.01	0.03
Period 9	−0.06	−0.01	−0.04	−0.09	0
HS 27 Mar 2009	−0.08	−0.1	−0.06	−0.09	−0.06
HS 25 May 2009	0.05	−0.06	0	−0.08	−0.1
HS 21 Oct 2009	−0.09	−0.05	−0.06	−0.12	−0.02
Curvature	**DHM 1 m**	**DHM 2 m**	**DHM 5 m**	**DHM 10 m**	**DHM 25 m**
Period 5	−0.09	−0.09	0	−0.15	−0.03
Period 1	−0.14	−0.18	−0.01	−0.21	−0.13
Period 2	0.03	0.12	0.02	0.14	0.1
Period 11	0.2	0.09	0	0.14	0.08
Period 9	−0.06	0.01	0	0.05	0.03
HS 27 Mar 2009	−0.17	−0.11	0	−0.2	−0.08
HS 25 May 2009	−0.06	0.11	−0.02	−0.07	−0.03
HS 21 Oct 2009	−0.32	−0.04	−0.01	−0.02	0.01
Roughness	**DHM 1 m**	**DHM 2 m**	**DHM 5 m**	**DHM 10 m**	**DHM 25 m**
Period 5	−0.13	−0.12	−0.05	−0.02	0.01
Period 1	0.1	0.13	0.17	0.14	−0.11
Period 2	−0.06	−0.08	−0.1	−0.08	0.01
Period 11	0.07	0.04	−0.02	−0.01	−0.01
Period 9	−0.04	−0.05	−0.05	0	−0.02
HS 27 Mar 2009	−0.13	−0.11	−0.03	0.01	0
HS 25 May 2009	−0.03	−0.11	−0.1	−0.12	0.21
HS 21 Oct 2009	−0.11	−0.11	−0.11	−0.07	−0.02

TCD
5, 1383–1418, 2011

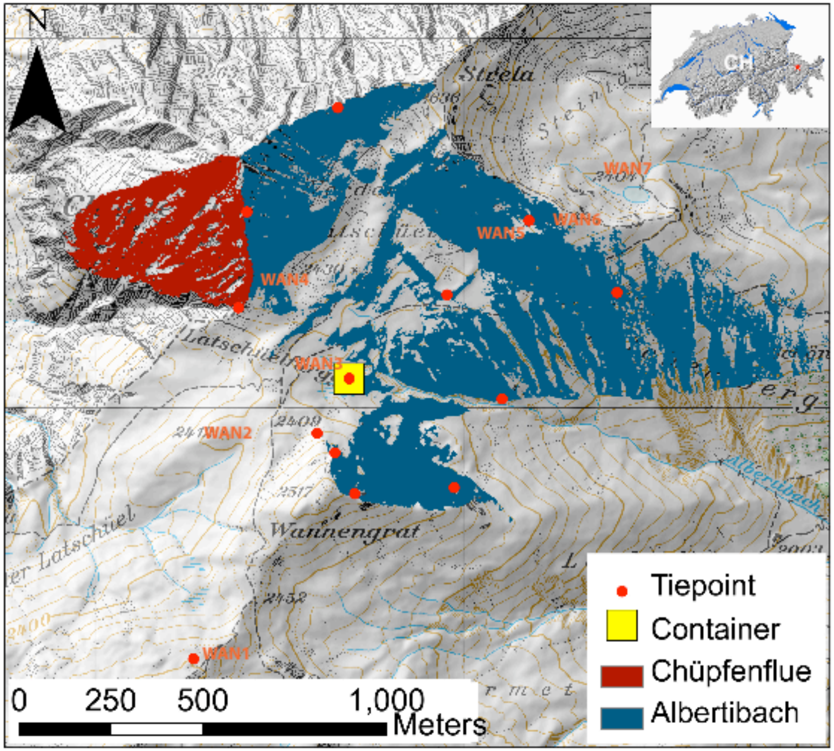

Fig. 1. Overview of the study site Wannengrat (region of Davos, Switzerland). Snow depths were measured with a terrestrial laser scanner (TLS) in the south-west face of the Chüpfenflue and in the catchment of Albertibach. The used equipment was stored in a container. To convert the TLS point-cloud into a Swiss coordinate system several fixed-installed reflectors (tie points) were used. Seven automatic weather stations (WAN1 to WAN7) deliver important additional information (e.g. temperature, wind-direction). For measurements in the Chüpfenflue the TLS was positioned next to the weather station WAN2.

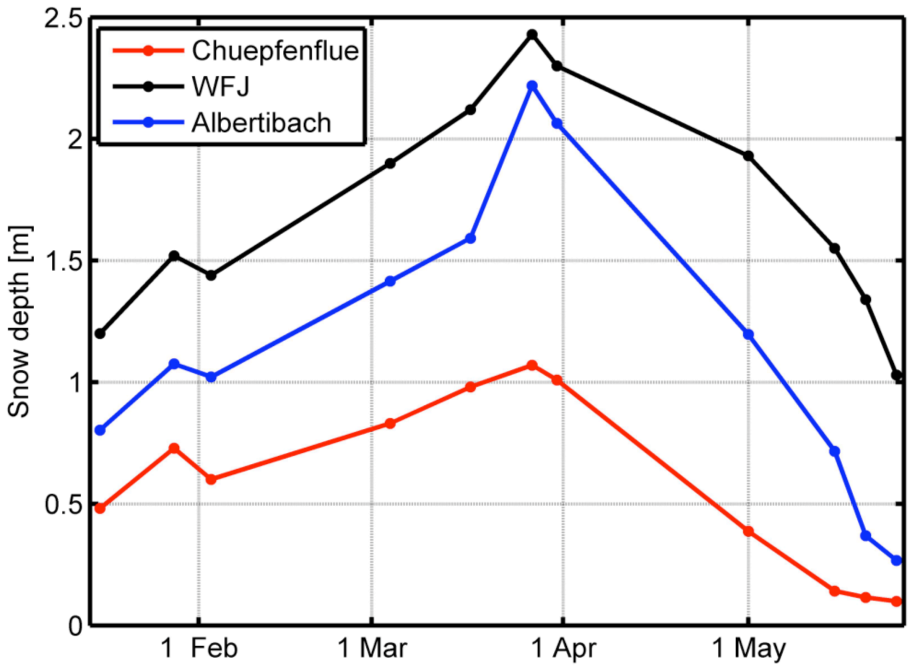

Fig. 2. Course of mean snow depth (HS_{tot}, calculated for the entire base area) of the rock face Chüpfenflue, of the Albertibach catchment and the measured snow depth at the Versuchsfeld Weissfluhjoch (WFJ) from 16 January to 25 May 2009.

TCD
5, 1383–1418, 2011

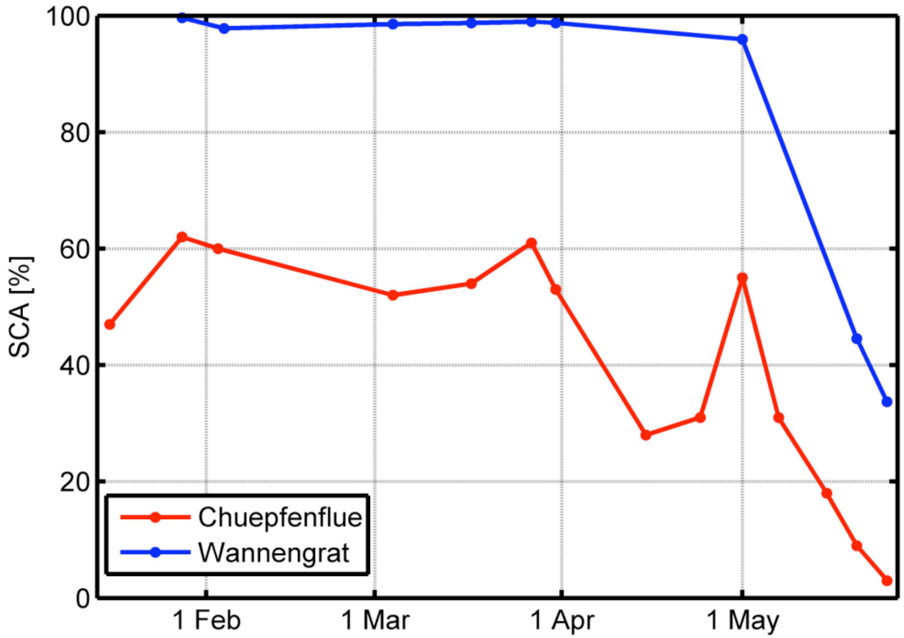

Fig. 3. Snow covered area (SCA) in the rock face Chüpfenflue and in the Albertibach catchment from 16 January to 25 May 2009. SCA was calculated for the entire base area.

TCD
5, 1383–1418, 2011

Spatio-temporal variability of snow depth in a rock face

V. Wirz et al.

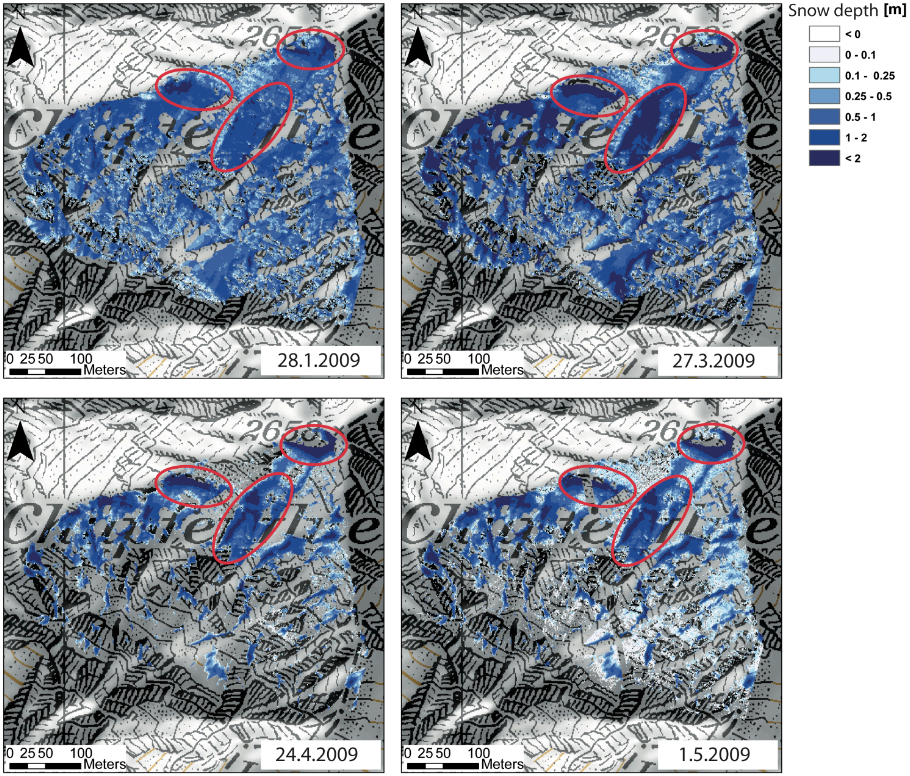

Fig. 4. Snow depth (HS) in the rock face Chüpfenflue in winter 2009. The red circles show areas with high HS during the entire winter.

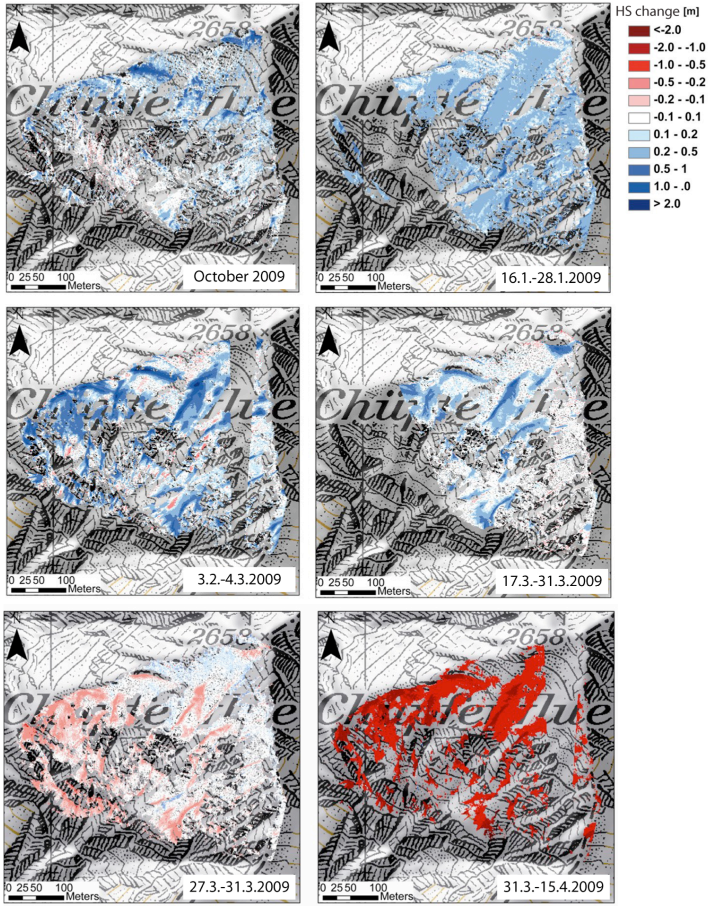

Fig. 5. Snow depth changes (dHS) during different observation periods in the rock face Chüpfenflue during the winter 2009 and of the first snow fall events of the winter 2009/2010 in October 2009.

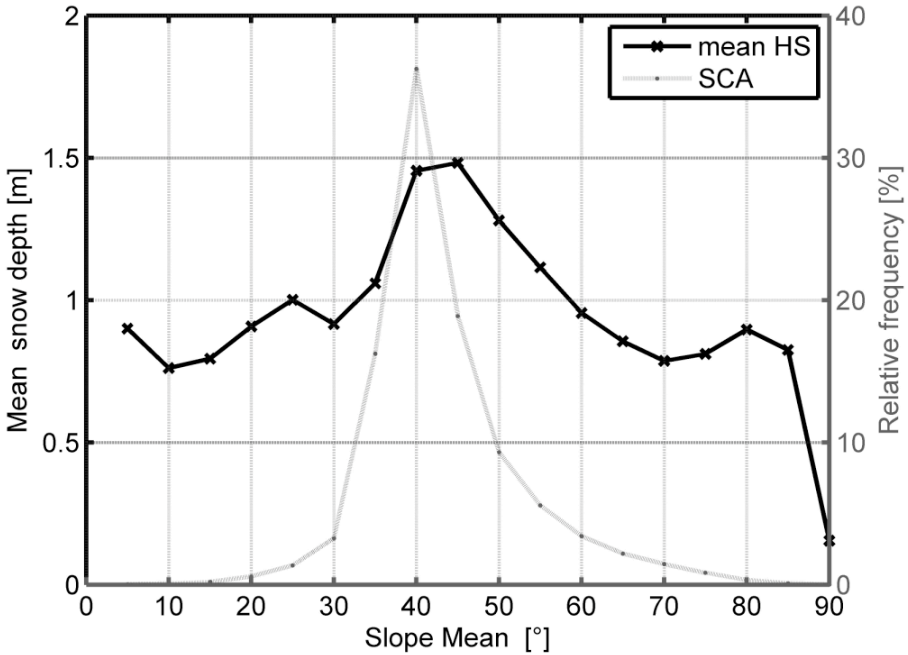

Fig. 6. Histogram (calculated for classes with a step width of 5° slope) of the mean sbow depth (HS, left axis) and the relative frequency of the snow covered cells (SCA) in the rock face Chüpfenflue on 27 March 2009.

TCD
5, 1383–1418, 2011

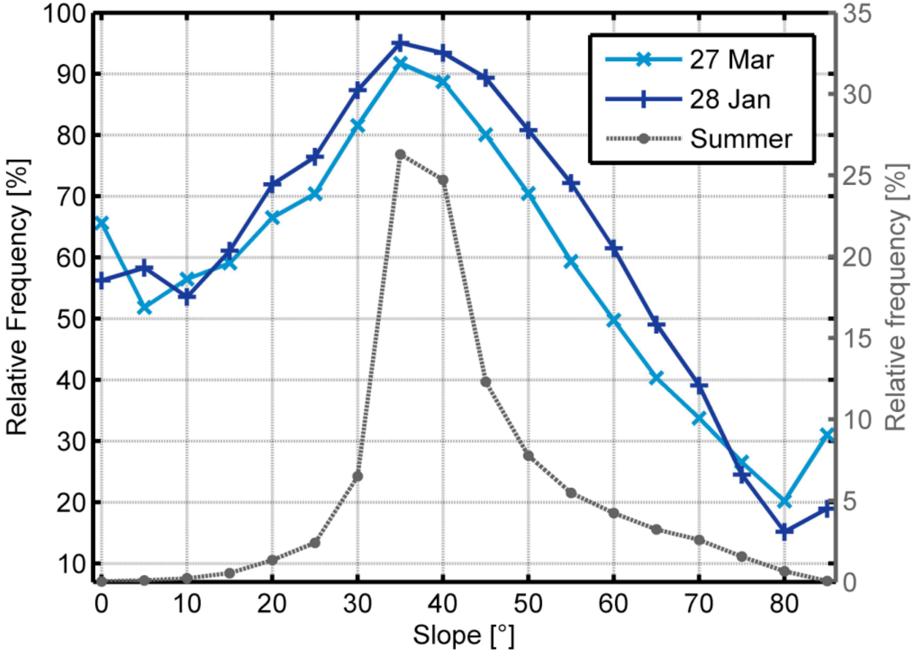

Fig. 7. The left axis shows the histogram with the relative frequencies of the snow covered cells per class (classes of cells with a step width of 5° slope) after a period with snowfall in combination with weak winds (28 January 2009), respectively in combination with strong northwest winds (27 March 2009). The right axis shows the histogram of the slope angle distribution in summer (based on DHM 1 m).

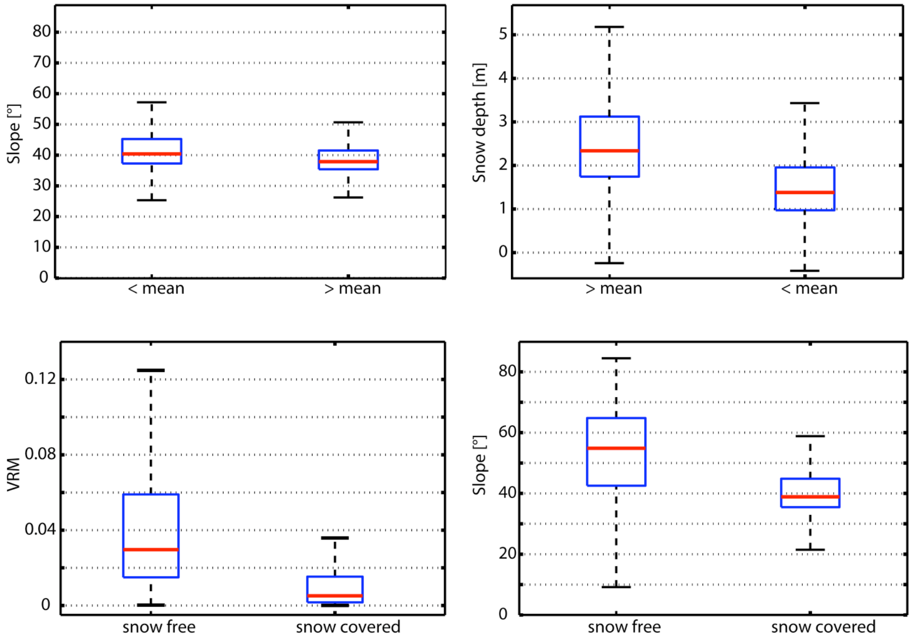

Fig. 8. Top: Boxplot to compare slope angle (left) and snow depth at the end of the accumulation season (HS_{max}, right) of cells with a snow depth change (dHS) higher than mean dHS (> mean) respectively smaller than mean dHS (< mean). dHS is given for period 7, ranging from 31 March to 15 April 2009. Bottom: Comparison of surface roughness (VRM, left) and slope angle (right) of the snow free, respectively snow covered area in the rock face Chüpfenflue at the end of the accumulation season (27 March 2009).